RSC Advances

RSC Publishing

PAPER

View Article Online
View Journal | View Issue

$CuFe_2O_4$ nanoparticles as a highly efficient and magnetically recoverable catalyst for the synthesis of medicinally privileged spiropyrimidine scaffolds†

Cite this: *RSC Advances*, 2013, **3**, 2924

Anshu Dandia,* Anuj K. Jain and Sonam Sharma

A highly efficient and green protocol for the synthesis of medicinally important fluorinated spiropyrimidine derivatives involving creation of six new covalent bonds has been developed using a magnetically separable and reusable heterogeneous copper ferrite nanocatalyst under mild reaction conditions. The synthesis of inverse spinel copper ferrite magnetic nanoparticles with average size of 38 nm has been achieved using combined sonochemical and co-precipitation techniques in aqueous medium from readily available inexpensive starting materials without any surfactant or capping agent. The particle size was determined by transmission electron microscopy (TEM), scanning electron microscopy (SEM) and X-ray diffraction (XRD) analysis. The magnetic nature of catalyst facilitates its easy removal from the reaction medium and can be reused five times without any significant loss of its catalytic activity. Negligible leaching of Cu and Fe in consecutive cycles makes the catalyst economical and environmentally benign. The structure of final products was established by single crystal X-ray analysis and spectroscopic techniques.

Received 10th October 2012,
Accepted 17th December 2012

DOI: 10.1039/c2ra22477a

www.rsc.org/advances

1. Introduction

In recent years, nanoscience is an emerging field in the search to exploit diverse technological applications and magnetic nanomaterials are envisaged to have a major impact in many areas, including biotechnology, environmental remediation and especially catalysis.[1] Nanoparticles have materialized as viable alternatives to conventional materials as robust, readily available, large-surface-area, fewer coordination sites, and reactive morphologies, which maximize the reaction rates and minimize consumption of the catalyst. In view of their nano-size, the contact between reactants and catalyst increases dramatically thus mimicking the heterogeneous catalyst. However, the recoverable problem must be addressed before nanocatalytic processes can be scaled-up, due to the fact that nanoparticles, which include nano-scaled metal catalysts and supports, are difficult to separate from the reaction mixture, which can lead to the blocking of filters and valves by the nanoparticle catalyst. Currently, a method used to address this problem is the use of magnetic nanoparticles (MNPs),[2] a route that has attracted wide research interest for its unique physical properties. They possess advantage of being magnetically recoverable, thereby eliminating the requirement for either solvent swelling before or catalyst filtration after completion of the reaction. The strategy of magnetic separation, taking advantage of MNPs, is typically more effective than filtration or centrifugation as it prevents loss of the catalyst. The magnetic separation of MNPs, is simple, economical and promising for industrial applications.

The increased interest in organofluorine compounds has led to the development of novel medicinal agents and new strategies in drug discovery and development. The synthesis of fluorine containing complexes or compounds and their derivatives provide unlimited potential for creating novel pharmacologically active lead compounds for use as therapeutics.[3] The selective introduction of one or more fluorine atoms or trifluormethyl group into specific positions in an organic molecule changes the molecules' physicochemical properties, including its stability, bioavailability, and lipophilicity. The above behavior could be explained by the unique physical, chemical, and biological properties of the fluorine atom.[4]

The hexahydropyrimidine skeleton is present in a number of alkaloids, eudistomidines H and I,[5] tetraponerines,[6] verbametrine[7] and verbamethine.[8] Hexetidine is a formaldehyde-releasing antimicrobial agent employed in mouthwashes and numerous products of veterinary and human drugs.[9] Different *N*-substituted hexahydropyrimidines are synthetic intermediates for spermidine-nitroimidazole drugs for the treatment of A549 lung carcinoma.[10] They form structural

Center for Advance Studies, Department of Chemistry, University of Rajasthan, Jaipur-302004, India. E-mail: dranshudandia@yahoo.co.in; Fax: +91 141 2609549; Tel: +91 941 4073436

† Electronic supplementary information (ESI) available. CCDC 897553. For ESI and crystallographic data in CIF or other electronic format see DOI: 10.1039/c2ra22477a

units in trypanothione reductase inhibiting ligands for the regulation of oxidative stress in parasite cells.[11] *N*-(4-aminobutyl) hexahydropyrimidine and *N*-(3-aminopropyl) hexahydropyrimidine are shown to compete with spermidine for uptake by L1210 cells.[12] Due to their significant biologically activity, hexahydropyrimidines have received a great deal of attention in recent years.

Hexahydropyrimidines are classically prepared by condensation between substituted propane-1,3-diamines and aldehydes or ketones.[13a–f] This method, however, limits the range of substitution at 5-position of the hexahydropyrimidines, being restrained by the availability of appropriately functionalized 1,3-diamines. There are also a few reports in the literature describing the synthesis of substituted hexahydropyrimidine derivatives by using α,β-unsaturated nitriles, by the reaction of substituted alanine and carbamide[14a,b] or by the reaction of 1,3-dicarbonyl compounds or cyclic ketones, aromatic amines and formaldehyde.[15a,b] Thus each of the known procedure has its own merits; however, further studies are still necessary for the versatile, simple, ecofriendly and economical multicomponent methodology.

Multicomponent reactions allow the creation of several bonds in a single operation and are attracting increasing attention as one of the most powerful emerging synthetic tools for the creation of molecular diversity and complexity.[16] Considering the above points and in continuation of our ongoing program in the development of greener and sustainable processes for heterocyclic synthesis[17] and nano-catalysis,[18,19] we were, thus, intrigued by the possibility of applying nanotechnology to the design of highly efficient, recyclable and magnetically recoverable $CuFe_2O_4$ nanoparticles as a heterogeneous catalyst for the synthesis of highly substituted spiropyrimidines incorporating pharmacophoric fluorine or trifluoromethyl group under mild reaction conditions for the first time.

2. Results and discussion

The first step entails the synthesis of highly stable copper ferrite nanoparticles. The catalyst was prepared by combined sonochemical and co-precipitation technique in aqueous medium without using any surfactant or capping agent. The nanostructure of $CuFe_2O_4$ nanoparticles has been well characterized by using X-ray diffraction (XRD), scanning electron microscopy (SEM) and transmission electron microscopy (TEM) technique. The crystallinity and phase purity of $CuFe_2O_4$ nanoparticles were examined by XRD measurements. As shown in Fig. 1, the strong and sharp reflection peaks in XRD patterns of dried precipitate which is mainly composed of tetragonal $CuFe_2O_4$ with a good crystallinity (JCPDS card N 034-0425).[20] The average particle size was calculated to be 38 nm using Scherrer formula,

$$D = 0.94\ \lambda/\beta\ \cos\theta$$

where D is the average size of the particles, λ is the wavelength of the incident X-ray, θ is the Bragg angle (in degrees), β is the full-width (in radians) subtended by the half-maximum intensity width of the powder peak, expressed in units of 2θ.

The structural composition and crystallinity of $CuFe_2O_4$ nanoparticles was further ascertained by SEM and TEM (Fig. 2 and 3). The EDX analysis showed that the distribution of the elements in the product was Cu = 14.28%, Fe = 28.95% and O = 56.77%. Thus the iron\copper ratio in the nanocrystals by EDX was found to be 2.02 which is very much close to the atomic ratio in the formula $CuFe_2O_4$. The particle size were also measured in SEM micrograph and were found to be in the range of 35–50 nm which is consistent with the particle size obtained from XRD analysis.

The FTIR spectra (Fig. S4, ESI†) of the $CuFe_2O_4$ nanoparticles indicate the presence of two absorption bands at 562 cm^{-1} and 480 cm^{-1}. These intense absorption bands are attributed to the stretching vibration of Fe^{3+}–O^{2-} in the

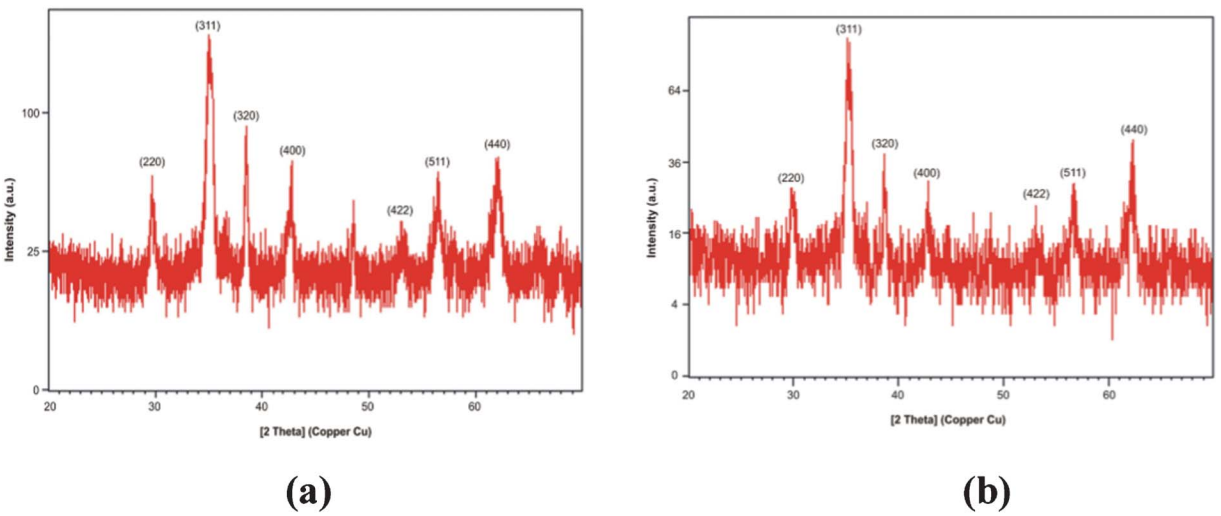

Fig. 1 (a) XRD spectrum of native $CuFe_2O_4$ catalyst. (b) XRD spectrum of reused $CuFe_2O_4$ catalyst after 4th cycle.

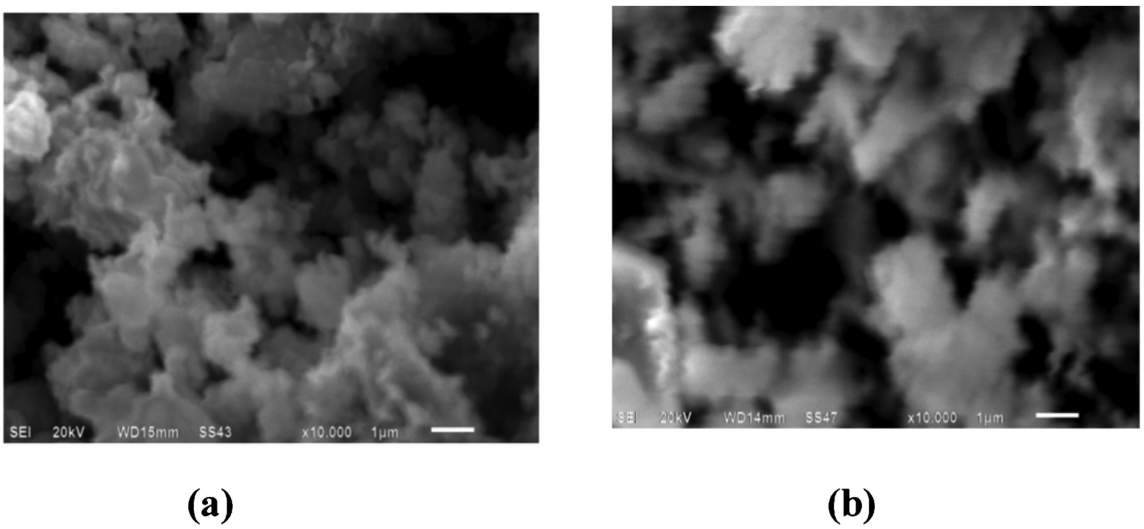

Fig. 2 (a) SEM image of native $CuFe_2O_4$ catalyst. (b) SEM image of reused $CuFe_2O_4$ catalyst after 4th cycle.

tetrahedral complexes and Cu^{2+}–O^{2-} in the octahedral complexes respectively. The positions of these bands confirm the existence of Cu^{2+} ions entirely in the octahedral sites and the Fe^{3+} ions in tetrahedral ones.[21]

The choice of an appropriate reaction medium is of crucial importance for successful synthesis. Initially, the three-component condensation reaction of cyclohexanone **1a**, formaldehyde **2** and 4-fluoroaniline **3a** in the presence of 10 mol% $CuFe_2O_4$ as a simple model substrate was investigated to establish the feasibility of the strategy and to optimize the reaction conditions (Scheme 1). Different solvents such as ethanol, acetonitrile, dimethyl sulfoxide (DMSO), DMF, dichloromethane, tetrahydrofuran and dioxane, were explored. After optimization, we observed that ethanol was the most effective solvent for this three-component condensation reaction. The use of ethanol effected not only the condensation reaction of ketone, formaldehyde and aromatic amine in good yield, but also performed well in the process of magnetic separation of nanoparticle catalysts, by reducing the viscosity of the reaction mixture and facilitating the congregation of magnetic catalyst, when the reaction was complete. Slightly lower yields were obtained when acetonitrile, dimethyl sulfoxide (DMSO), and DMF were used as the solvent (Table 1, entries 3, 4 and 5). Dichloromethane, tetrahydrofurane and dioxane afforded the products in only low to moderate yields (Table 1, entries 6–8). The corresponding product was also obtained in good yield under neat conditions (Table 1, entry 9). However, the mixture was viscous in the absence of a solvent and made the separation of catalyst from products difficult magnetically unless an extraction solvent such as ether was added. Performing the reaction with a higher catalyst loading (20 mol%) had no significant effect on yield. However, if the amount of the catalyst was reduced to 5 and 1 mol%, the product yield was reduced to 62% and 26% respectively.

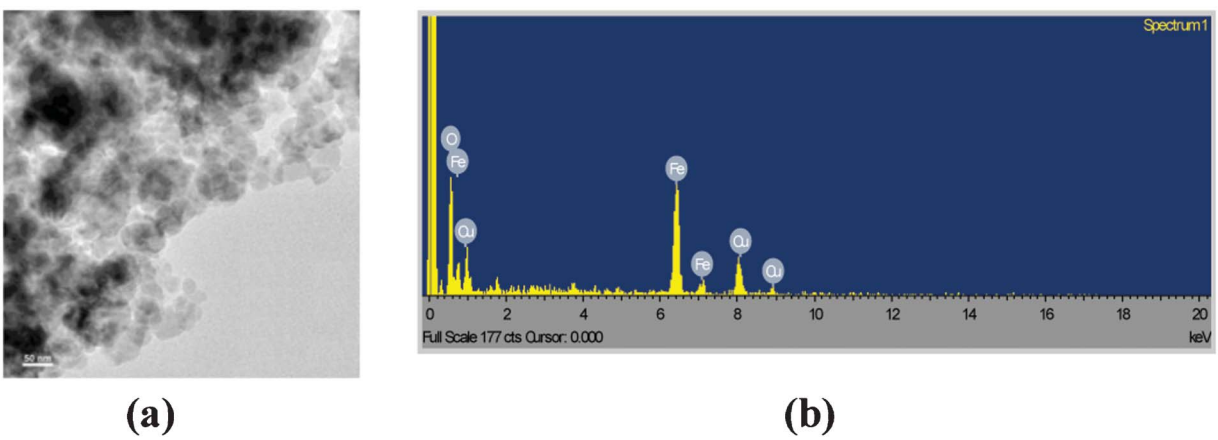

Fig. 3 (a) TEM image of native $CuFe_2O_4$ catalyst. (b) The EDX spectrum of native $CuFe_2O_4$ catalyst.

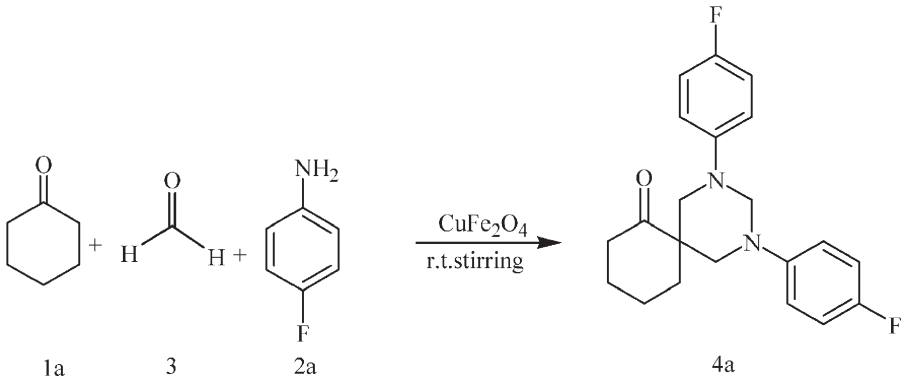

Scheme 1 Synthesis of spirohexahydropyrimidine **4a**.

The $CuFe_2O_4$ nanoparticle catalyst plays a crucial role in the success of the reaction. In the absence of $CuFe_2O_4$ nanoparticle catalyst, the model reaction (Scheme 1) could be carried out, but the product was obtained in very low yield after prolonged reaction time (Table 1, entry 1).

With these encouraging results in hand, we turned to explore the scope of the reaction using different aromatic amines as substrates under the optimized reaction conditions (Table 2). It was observed that the aromatic amines having electron donating as well as electron withdrawing group reacted successfully to furnish spiropyrimidine derivatives with good yields. In addition, we have also explored the reactivity of cyclic ketones for this transformation. From the results, it is clear that cyclohexanone showed better reactivity than 4-methylcyclohexanone and slightly higher yields were obtained, while, 1,4-dioxaspiro[4.5]decan-8-one is found to be less active than cyclohexanone (Table 2).

Further, the leaching of the metal from the $CuFe_2O_4$ nanoparticles was investigated. After completion of the reaction, the supernatant was collected and tested for Fe and Cu by inductively coupled plasma-atomic emission spectroscopy (ICP-AES). The leaching of Fe and Cu in three consecutive cycles was found to be $\leqslant 0.5$ ppm, which is well below the permissible level concerning the toxicity in humans.[22] This study clearly demonstrated that there was no significant amount of leaching. It is also observed from spectral studies that there is no change in the nature of the catalyst even after four cycles. The powder X-ray diffraction analysis exhibited identical peaks for both fresh and recovered $CuFe_2O_4$ nanoparticles, which were compared with those reported in the literature (Fig. 1).[20] In addition, the SEM analysis of $CuFe_2O_4$ nanoparticles before and after the reaction showed identical shape and size (Fig. 2). These experimental results clearly suggest that there was no significant change in the catalytic activity of nano-$CuFe_2O_4$ before and after the reaction.

The proposed mechanism for the formation of spirohexahydropyrimidine derivatives is shown in Scheme 2. Initially an imine is formed due to nucleophilic addition of aromatic amine to formaldehyde and subsequent loss of water molecule. After the imine formation, *in situ* generated enolate attacks imine to afford β-amino carbonyl derivative A. Intermediate A reacts further in the same manner to form substituted propane-1,3-diamine B. Finally the condensation of the resulting substituted propane-1,3-diamine B with formaldehyde furnishes the desired spirohexahydropyrimidines.

Here, oxide (O^{2-}) of the metal oxide framework acting as a Lewis base and Fe^{3+} as Lewis acid coordinate with the carbonyl oxygen, thus increasing the electrophilicity of the carbonyl carbon and thereby making it possible to carry out the reaction at room temperature in short reaction time.

The reusability of the nano-$CuFe_2O_4$ catalyst was examined and the results are summarized in Table 3. The catalyst was magnetically separated from the reaction mixture after completion of the reaction, washed with ethanol, air dried and used directly for further catalytic reactions. No significant loss of catalyst ($CuFe_2O_4$) activity was observed up to four cycles.

All the products were well characterized by IR, ^1H, ^{13}C NMR, mass spectra and elemental analysis. The final structure was confirmed by single crystal X-ray analysis of 9,11-bis-(4-fluorophenyl)-1,4-dioxa-9,11-diazadispiro [4.1.5.3]pentadecan-13-one (**4k**) (Fig. 4).[23]

Table 1 Optimization for the synthesis of **4a**

Entry	Solvents	$CuFe_2O_4$ (mol%)	Time (h)	Yield (%)[a]
1	Ethanol	—	24	14
2	Ethanol	10	3	82
3	Acetonitrile	10	4	70
4	DMSO	10	4	76
5	DMF	10	4	75
6	Dichloromethane	10	5	67
7	Tetrahydrofuran	10	5	58
8	Dioxane	10	4	39
9	Neat	10	3	82
10	Ethanol	20	3	83
11	Ethanol	5	3	62
12	Ethanol	1	4	26

[a] Isolated yield.

Table 2 Synthesis of spirohexahydropyrimidines

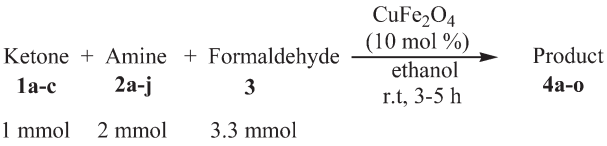

Entry	Ketone	Amine	Product	Time (h)	Yield(%)[a]	MP (°C)
1	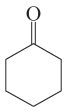	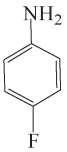	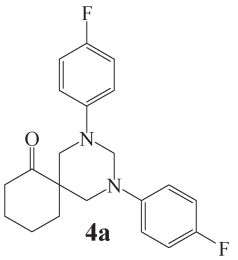 **4a**	3	82	122–124
2	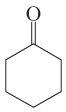	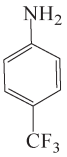	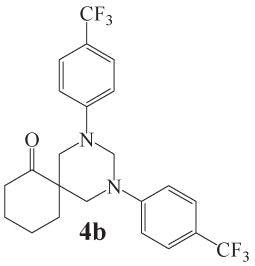 **4b**	4	73	178–180
3	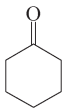	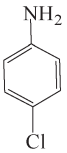	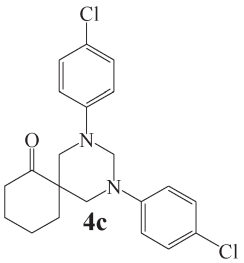 **4c**	3	79	160–162
4	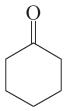	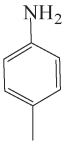	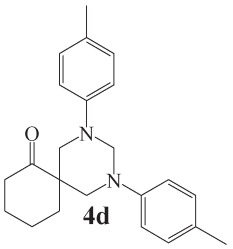 **4d**	4	74	124–126
5	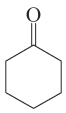	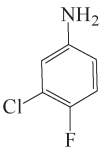	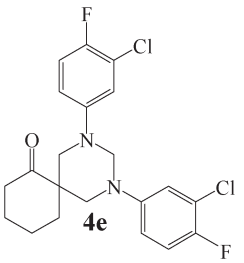 **4e**	4	75	248–250

Table 2 (*Continued*)

Entry	Ketone	Amine	Product	Time (h)	Yield(%)[a]	MP (°C)
6	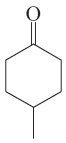	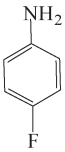	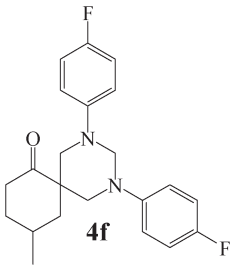 **4f**	4	76	130–132
7	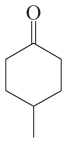	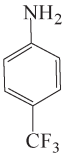	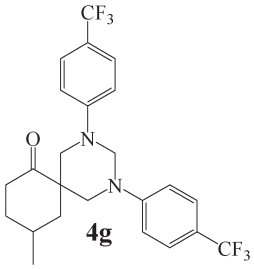 **4g**	4.5	70	204–206
8	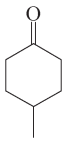	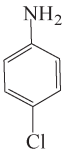	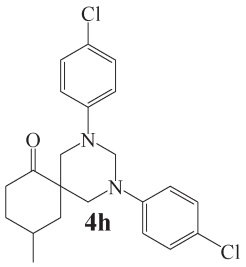 **4h**	4	75	166–168
9	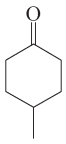	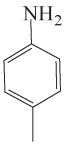	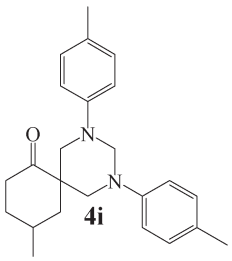 **4i**	4	72	104–106
10	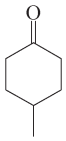	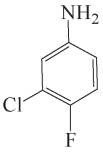	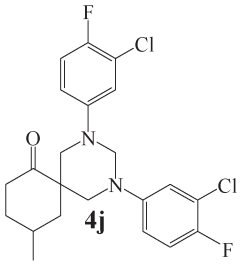 **4j**	4	64	236–238

Table 2 (*Continued*)

Entry	Ketone	Amine	Product	Time (h)	Yield(%)[a]	MP (°C)
11	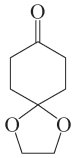	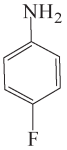	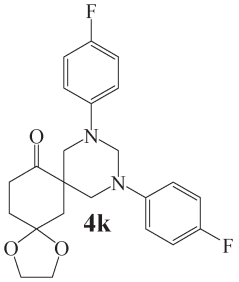 **4k**	4	58	130–132
12	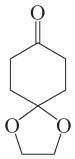	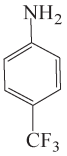	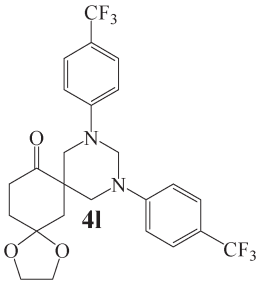 **4l**	4.5	54	144–146
13	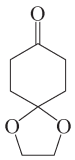	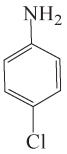	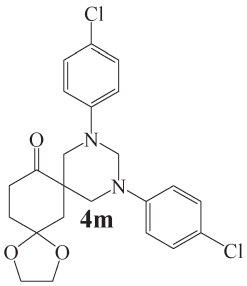 **4m**	4	61	132–134
14	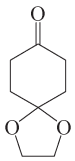	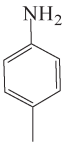	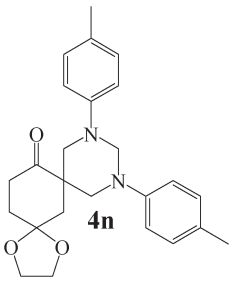 **4n**	4.5	52	126–128
15	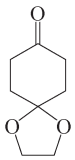	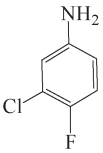	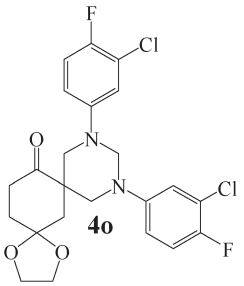 **4o**	5	55	206–208

[a] Isolated yield.

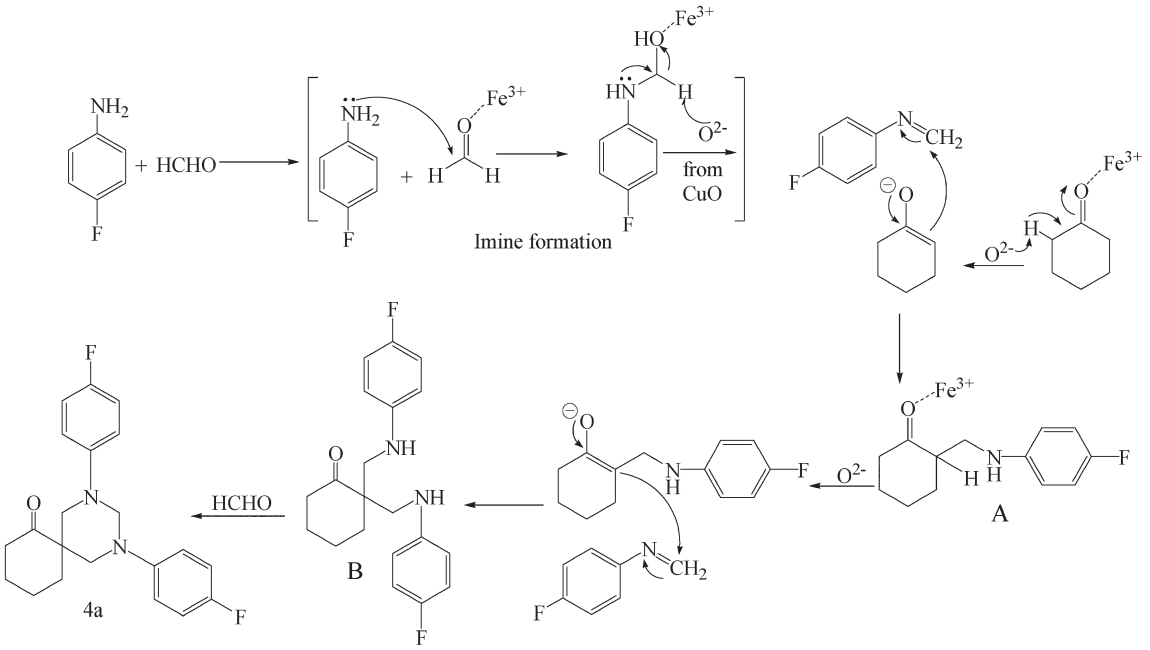

Scheme 2 Plausible mechanism for the reaction of 4-fluoroaniline and formaldehyde with cyclohexanone.

3. Experimental

3.1 General

All the chemicals used were of research grade and were used without further purification. The melting points of all compounds were determined on a Toshniwal apparatus. The purity of compounds was checked on thin layers of silica Gel–G coated glass plates and n-hexane : ethyl acetate (8 : 2) as eluent. IR spectra were recorded on a Shimadzu FT IR–8400S spectrophotometer using KBr pellets. ^{1}H and ^{13}C NMR spectra were recorded in $CDCl_3$ using TMS as an internal standard on a Bruker spectrophotometer at 300 and 75 MHz respectively. Mass spectra of representative compounds were recorded on JEOL-SX-102 mass spectrometer at 70 eV. Elemental microanalyses were carried out on a Carlo-Erba 1108 CHN analyzer. Single crystal X-ray diffraction was performed on a Bruker Kappa Apex II instrument.

3.2 Preparation $CuFe_2O_4$ nanoparticles

$CuFe_2O_4$ nanoparticles were prepared by thermal decomposition of $Cu(NO_3)_2$ and $Fe(NO_3)_3$ in water in the presence of sodium hydroxide. Briefly, to a solution of $Fe(NO_3)_3{\cdot}9H_2O$ (3.34 g, 8.2 mmol) and $Cu(NO_3)_2{\cdot}3H_2O$ (1 g, 4.1 mmol) in 75 mL of distilled water, 3 g (75 mmol) of NaOH dissolved in 15 mL of water was added at room temperature over a period of 10 min during which a reddish-black precipitate was formed. Then the reaction mixture was warmed to 90 °C and stirred under ultrasonic irradiation for two hours. After 2 h, it was cooled to room temperature and the magnetic particles so formed were separated by a magnetic separator. It was then washed with water (3 × 30 mL) and catalyst was kept in an air oven for overnight at 80 °C. Then the catalyst was ground in a mortar-pestle and kept in a furnace at 700 °C for 5 h (step up temperature 20 °C min^{-1}) and then cooled to room tempera-

Table 3 Reusability of the nano-$CuFe_2O_4$ catalyst for the synthesis of **4a**

No. of cycles	Yield (%)[a]
1	82
2	81
3	80
4	79
5	79

[a] Isolated yields.

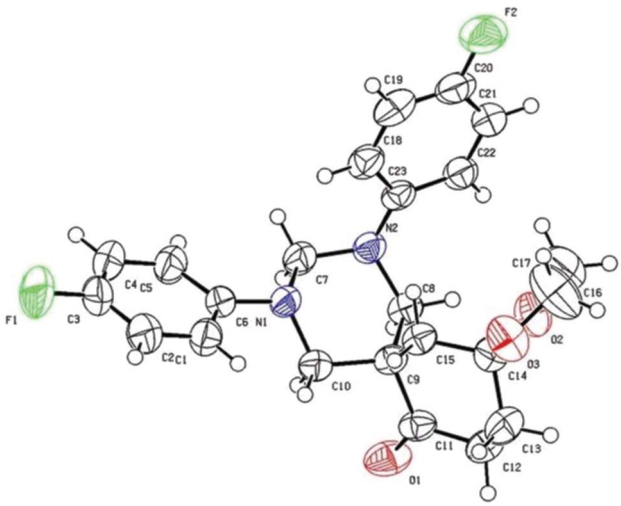

Fig. 4 Single crystal X-ray structure of 9,11-bis-(4-fluorophenyl)-1,4-dioxa-9,11-diazadispiro[4.1.5.3]pentadecan-13-one (**4k**).

ture. 930 mg of magnetic $CuFe_2O_4$ particles of size 35–50 nm were obtained.

3.3 Catalyst characterization

The wide angle X-ray diffraction pattern of the sample was obtained using Bragg–Brentanno geometry on PANalytical X′pert pro diffractometer in 2θ range of 20–70° with Cu-Kα radiation source (λ = 1.5406 Å). The X-ray tube was operated at 45 kV and 40 mA. TEM measurements of the sample were carried out using a JEOL transmission electron microscope. Sample for the TEM was prepared by making a clear dispersion of nanoparticles in dimethyl formaldehyde and putting a drop of it on a carbon-coated copper grid. Formation of copper ferrite nanoparticles was first ascertained by electron dispersive X-ray (EDX) analysis combined with scanning electron microscopy (SEM). SEM was done on a 'JEOL JSM-6610LV' Scanning Electron Microscope combined with EDX system (INCA Analyzer). For SEM analysis, the sample was dispersed on the aluminium stub used for sample mounting. The sample was scanned at an accelerating voltage of 20 kV at a working distance of 15 mm. The particle size was measured at a magnification of 10 kX.

3.4 General procedure for the synthesis of spiropyrimidine derivatives 4(a–o)

To a solution of cyclic ketones (1 mmol), aromatic amines (2 mmol), formaldehyde (3.3 mmol, 36% aqueous solution), and a catalytic amount of $CuFe_2O_4$ (10 mol%) in ethanol (5 mL) was stirred at room temperature for the stipulated times. After completion of the reaction monitored by TLC, 10 mL ethanol was added to the reaction mixture and the catalyst $CuFe_2O_4$ was separated magnetically. The reaction mixture was allowed to stand overnight. The solid material was filtered off, washed with water (2 × 10 mL), dried and recrystallized from ethanol to furnish pure spiropyrimidine derivatives.

Spectral data of compounds 4(a–o). (**4a**) 2,4-Bis-(4-fluorophenyl)-2,4-diazaspiro[5.5]undecan-7-one. White solid; (Yield: 82%); mp 122–124 °C; IR (KBr): 2944, 2785, 1712, 1576, 1486, 1233, 1208, 827 cm^{-1}; ^1H NMR (300 MHz, $CDCl_3$): δ 1.70–1.64 (m, 2H), 1.87–1.84 (m, 4H), 2.36 (t, J = 6.3 Hz, 2H), 3.50–3.37 (q, J = 12.6 Hz, 4H), 4.15 (d, J = 11.4 Hz, 1H), 4.61 (d, J = 11.1 Hz, 1H), 7.00–6.97 (m, 8H, ArH), ^{13}C NMR (75 MHz, $CDCl_3$): 20.8, 27.8, 35.0, 39.1, 49.9, 56.2, 70.1, 115.6, 115.9, 119.2, 146.2, 156.0, 159.2, 212.8; MS (ESI) m/z: 356 $[M]^+$. Anal. Calcd for $C_{21}H_{22}F_2N_2O$: C, 70.77; H, 6.22; N, 7.86. Found: C, 70.65; H, 6.17; N, 8.05.

(**4b**) 2,4-Bis-(4-trifluoromethylphenyl)-2,4-diazaspiro[5.5]undecan-7-one. White solid; (Yield: 73%); mp 178–180 °C; IR (KBr): 2958, 2802, 1716, 1562, 1498, 1236, 1222, 816 cm^{-1}; ^1H NMR (300 MHz, $CDCl_3$): δ 1.76–1.69 (m, 2H), 1.93–1.88 (m, 4H), 2.42 (t, J = 6.6 Hz, 2H), 3.63 (m, 4H), 4.19 (d, J = 11.1 Hz, 1H), 4.60 (d, J = 11.7 Hz, 1H), 7.32–6.95 (m, 8H, ArH), ^{13}C NMR (75 MHz, $CDCl_3$): 21.2, 27.5, 34.3, 41.8, 49.5, 55.4, 69.9, 112.7, 113.2, 117.6, 145.9, 153.5, 159.8, 211.3; MS (ESI) m/z: 456 $[M]^+$. Anal. Calcd for $C_{23}H_{22}F_6N_2O$: C, 60.52; H, 4.86; N, 6.14. Found: C, 60.58; H, 4.72; N, 6.04.

(**4c**) 2,4-Bis-(4-chlorophenyl)-2,4-diazaspiro[5.5]undecan-7-one. White solid; (Yield: 79%); mp 160–162 °C; IR (KBr): 2948, 2782, 1708, 1592, 1488, 1232, 1216, 828 cm^{-1}; ^1H NMR (300 MHz, $CDCl_3$): δ 1.71–1.67 (m, 2H), 1.90–1.86 (m, 4H), 2.37 (t, J = 6.3 Hz, 2H), 3.51 (l, 4H), 4.22 (d, J = 11.4 Hz, 1H), 4.74 (d, J = 11.4 Hz, 1H), 6.98 (d, J = 7.2 Hz, 4H), 7.24 (d, J = 10.2 Hz, 4H), ^{13}C NMR (75 MHz, $CDCl_3$): 20.8, 27.6, 34.7, 39.1, 49.9, 55.2, 67.9, 118.2, 125.2, 129.1, 148.3, 212.5; MS (ESI) m/z: 389 $[M]^+$. Anal. Calcd for $C_{21}H_{22}Cl_2N_2O$: C, 64.79; H, 5.70; N, 7.20. Found: C, 64.88; H, 5.77; N, 7.08.

(**4d**) 2,4-Di-*p*-tolyl-2,4-diazaspiro[5.5]undecan-7-one. White solid; (Yield: 74%); mp 124–126 °C; IR (KBr): 2932, 1708, 1546, 1460, 1234, 1210, 816 cm^{-1}; ^1H NMR (300 MHz, $CDCl_3$): δ 1.68–1.66 (m, 2H), 1.88–1.86 (m, 4H), 2.29 (s, 6H), 2.39 (t, J = 6.0 Hz, 2H), 3.40 (d, J = 12.3 Hz, 2H), 3.52 (d, J = 12.6 Hz, 2H), 4.10 (d, J = 11.4 Hz, 1H), 4.79 (d, J = 11.1 Hz, 1H), 6.96 (d, J = 8.1 Hz, 4H), 7.10 (d, J = 8.1 Hz, 4H), ^{13}C NMR (75 MHz, $CDCl_3$): 20.4, 20.8, 27.7, 29.6, 34.6, 39.1, 50.0, 55.4, 69.4, 117.4, 129.7, 147.8, 213.3; MS (ESI) m/z: 348 $[M]^+$. Anal. Calcd for $C_{23}H_{28}N_2O$: C, 79.27; H, 8.10; N, 8.04. Found: C, 79.41; H, 8.21; N, 7.95.

(**4e**) 2,4-Bis-(3-chloro-4-fluorophenyl)-2,4-diazaspiro[5.5]undecan-7-one. White solid; (Yield: 75%); mp 248–250 °C; IR (KBr): 2948, 2782, 1708, 1592, 1488, 1232, 1216, 828 cm^{-1}; ^1H NMR (300 MHz, $CDCl_3$): δ 1.72–1.69 (m, 2H), 1.99–1.81 (m, 4H), 2.46 (t, J = 6.9 Hz, 2H), 3.35 (d, J = 12.6 Hz, 2H), 3.59 (d, J = 12.6 Hz, 2H), 4.28 (d, J = 11.4 Hz, 1H), 4.71 (d, J = 11.4 Hz, 1H), 6.87 (d, J = 8.4 Hz, 2H), 6.92 (s, 2H), 7.24 (d, J = 8.7 Hz, 2H), ^{13}C NMR (75 MHz, $CDCl_3$): 20.3, 27.9, 34.8, 39.2, 50.8, 55.4, 69.3, 114.4, 119.9, 129.2, 131.6, 135.5, 148.7, 213.3; MS (ESI) m/z: 425 $[M]^+$. Anal. Calcd for $C_{21}H_{20}Cl_2F_2N_2O$: C, 59.31; H, 4.74; N, 6.59. Found: C, 59.19; H, 4.82; N, 6.69.

(**4f**) 2,4-Bis-(4-fluorophenyl)-10-methyl-2,4-diazaspiro[5.5]undecan-7-one. White solid, (Yield: 76%); mp 130–132 °C; IR (KBr): 2978, 2922, 2863, 1712, 1609, 1498, 1474, 1256, 1126, 1026, 912, 806, 744 cm^{-1}; ^1H NMR (300 MHz, $CDCl_3$): δ 0.83 (d, J = 6.0 Hz, 3H), 1.06 (t, J = 12.6 Hz, 1H), 1.41–1.31 (m, 1H), 2.00 (br s, 2H), 2.37–2.22 (m, 2H), 2.57–2.45 (m, 1H), 3.03 (d, J = 12.3 Hz, 1H), 3.30 (d, J = 12.6 Hz, 1H), 3.61 (d, J = 12.6 Hz, 1H), 3.75 (d, J = 12.6 Hz, 1H), 4.14 (d, J = 11.4 Hz, 1H), 4.62 (d, J = 11.1 Hz, 1H), 7.00–6.98 (m, 8H), ^{13}C NMR (75 MHz, $CDCl_3$): 21.2, 27.3, 35.7, 38.6, 43.1, 49.3, 56.0, 57.1, 70.2, 115.6, 115.9, 118.9, 119.0, 119.6, 146.2, 156.1, 159.1, 213.0; MS (ESI) m/z: 370 $[M]^+$. Anal. Calcd for $C_{22}H_{24}F_2N_2O$: C, 71.33; H, 6.53; N, 7.56. Found: C, 71.60; H, 6.58; N, 7.35.

(**4g**) 2,4-bis-(4-trifluoromethylphenyl)-10-methyl-2,4-diazaspiro[5.5]undecan-7-one. White solid, (Yield: 70%); mp 204–206 °C; IR (KBr): 2972, 2934, 2855, 1710, 1617, 1532, 1463, 1222, 1138, 1018, 922, 806, 738 cm^{-1}; ^1H NMR (300 MHz, $CDCl_3$): δ 0.92 (d, J = 6.6 Hz, 3H), 1.05 (t, J = 12.0 Hz, 1H), 1.63–1.58 (m, 1H), 2.13–2.01 (m, 2H), 2.58–2.52 (m, 3H), 3.24 (d, J = 12.3 Hz, 1H), 3.48 (d, J = 12.9 Hz, 1H), 3.68 (d, J = 11.7 Hz, 1H), 3.82 (d, J = 12.3 Hz, 1H), 4.21 (d, J = 11.7 Hz, 1H), 4.69 (d, J = 11.7 Hz, 1H), 7.11 (d, J = 8.1 Hz, 4H), 7.29 (d, J = 8.4 Hz, 4H), ^{13}C NMR (75 MHz, $CDCl_3$): 21.8, 27.1, 37.7, 39.4, 42.1, 50.5, 55.9, 57.6, 69.4, 115.3, 118.1, 123.5, 127.1, 130.2, 135.6, 142.4, 150.9, 212.5; MS (ESI) m/z: 470 $[M]^+$. Anal. Calcd for $C_{24}H_{24}F_6N_2O$: C, 61.27; H, 5.14; N, 5.95. Found: C, 61.50; H, 5.18; N, 5.78.

(**4h**) 2,4-bis-(4-chlorophenyl)-10-methyl-2,4-diazaspiro[5.5]undecan-7-one. White solid, (Yield: 75%); mp 166–168 °C; IR (KBr): 2960, 2928, 2860, 1704, 1618, 1502, 1462, 1240, 1126,

1014, 910, 814, 736 cm^{-1}; ^1H NMR (300 MHz, $CDCl_3$): δ 0.85 (d, J = 6.3 Hz, 3H), 1.09 (t, J = 12.6 Hz, 1H), 2.04–1.98 (m, 3H), 2.35–2.28 (m, 2H), 2.51–2.49 (m, 1H), 3.14 (d, J = 12.9 Hz, 1H), 3.39 (d, J = 12.6 Hz, 1H), 3.71 (d, J = 12.6 Hz, 1H), 3.84 (d, J = 12.9 Hz, 1H), 4.25 (d, J = 11.4 Hz, 1H), 4.75 (d, J = 11.7 Hz, 1H), 7.06–6.98 (m, 4H), 7.27–7.23 (m, 4H), ^{13}C NMR (75 MHz, $CDCl_3$): 21.2, 27.4, 35.6, 38.6, 42.9, 49.4, 55.0, 56.1, 68.1, 118.0, 118.6, 125.0, 125.6, 129.1, 129.2, 148.3, 212.6; MS (ESI) m/z: 403 $[M]^+$. Anal. Calcd for $C_{22}H_{24}Cl_2N_2O$: C, 65.51; H, 6.00; N, 6.95. Found: C, 65.42; H, 6.07; N, 6.82.

(**4i**) 10-Methyl-2,4-di-*p*-tolyl-2,4-diazaspiro[5.5]undecan-7-one. White solid, (Yield: 72%); mp 104–106 °C; IR (KBr): 2962, 2926, 1710, 1614, 1520, 1456, 1388, 1224, 1136, 918, 816, 732, 524 cm^{-1}; ^1H NMR (300 MHz, $CDCl_3$): δ 0.79 (d, J = 5.6 Hz, 3H), 1.03 (t, J = 12.8 Hz, 1H), 1.42–1.25 (m, 1H), 1.99–1.94 (m, 2H), 2.28–2.22 (l, 7H), 2.42–2.38 (m, 1H), 2.60–2.49 (m, 1H), 3.16 (d, J = 12.6 Hz, 1H), 3.21 (d, J = 12.6 Hz, 1H), 3.56 (d, J = 12.6 Hz, 1H), 3.82 (d, J = 12.6 Hz, 1H), 4.10 (d, J = 11.4 Hz, 1H), 4.78 (d, J = 11.4 Hz, 1H), 6.88–6.83 (m, 4H), 7.11 (d, J = 9.2 Hz, 4H), ^{13}C NMR (75 MHz, $CDCl_3$): 20.5, 21.0, 27.3, 35.4, 37.1, 43.1, 49.8, 55.0, 56.9, 70.3, 116.7, 117.6, 129.5, 130.3, 147.9, 212.8; MS (ESI) m/z: 362 $[M]^+$. Anal. Calcd for $C_{24}H_{30}N_2O$: C, 79.52; H, 8.34; N, 7.73. Found: C, 79.63; H, 8.26; N, 7.62.

(**4j**) 2,4-Bis-(3-chloro-4-fluorophenyl)-10-methyl-2,4-diazaspiro[5.5]undecan-7-one. White solid, (Yield: 64%); mp 236–238 °C; IR (KBr): 2960, 2928, 2860, 1704, 1618, 1502, 1462, 1240, 1126, 1014, 910, 814, 736 cm^{-1}; ^1H NMR (300 MHz, $CDCl_3$): δ 0.91 (d, J = 6.9 Hz, 3H), 1.03 (t, J = 12.6 Hz, 1H), 1.68–1.61 (m, 1H), 2.04–1.98 (m, 2H), 2.51–2.45 (m, 3H), 3.29 (d, J = 12.3 Hz, 2H), 3.54 (d, J = 12.3 Hz, 1H), 3.83 (d, J = 12.3 Hz, 1H), 4.21 (d, J = 11.1 Hz, 1H), 4.73 (d, J = 11.1 Hz, 1H), 6.81–6.74 (m, 2H), 6.91(s, 2H), 7.19 (d, J = 8.4 Hz, 2H), ^{13}C NMR (75 MHz, $CDCl_3$): 21.9, 27.8, 36.2, 39.7, 42.9, 50.3, 55.1, 56.8, 67.4, 115.3, 118.8, 120.5, 124.1, 130.5, 136.7, 151.3, 212.6; MS (ESI) m/z: 439 $[M]^+$. Anal. Calcd for $C_{22}H_{22}Cl_2F_2N_2O$: C, 60.15; H, 5.05; N, 6.38. Found: C, 60.03; H, 5.14; N, 6.27.

(**4k**) 2,4-Bis(4-fluorophenyl)-10-(1,1-dioxa-2,2-dimethylene)-2,4-diazaspiro[5.5]undecan-7-one. White solid, (Yield: 58%); mp 130–132 °C; IR (KBr): 2988, 1704, 1528, 1445, 1256, 1047, 932, 830, 718 cm^{-1}; ^1H NMR (300 MHz, $CDCl_3$): δ 2.02 (t, J = 6.9 Hz, 2H), 2.14 (s, 2H), 2.57 (t, J = 6.6 Hz, 2H), 3.30 (d, J = 12.3 Hz, 2H), 3.92–3.66 (m, 6H), 4.00 (d, J = 10.8 Hz, 1H), 4.72 (d, J = 11.1 Hz, 1H), 6.99–6.97 (m, 8H), ^{13}C NMR (75 MHz, $CDCl_3$): 35.0, 36.3, 40.5, 48.7, 57.0, 64.4, 69.8, 107.1, 115.5, 115.8, 119.2, 146.4, 155.9, 159.1, 211.4; MS (ESI) m/z: 414 $[M]^+$. Anal. Calcd for $C_{23}H_{24}F_2N_2O_3$: C, 66.65; H, 5.84; N, 6.76. Found: C, 66.82; H, 5.77; N, 6.48.

(**4l**) 2,4-Bis(4-trifluoromethylphenyl)-10-(1,1-dioxa-2,2-dimethylene)-2,4-diazaspiro[5.5]undecan-7-one. White solid, (Yield: 54%); mp 144–146 °C; IR (KBr): 2954, 1708, 1512, 1456, 1244, 1042, 918, 826, 726 cm^{-1}; ^1H NMR (300 MHz, $CDCl_3$): δ 2.13–2.01 (m, 4H), 2.43–2.37 (m, 1H), 2.97–2.65 (m, 4H), 3.22–3.16 (m, 1H) 3.44–3.37 (m, 2H), 4.05–4.02 (m, 4H), 6.57 (d, J = 8.7 Hz, 4H), 7.37 (d, J = 8.7 Hz, 4H), ^{13}C NMR (75 MHz, $CDCl_3$): 34.4, 38.3, 38.7, 43.0, 46.0, 48.9, 64.7, 64.8, 107.0, 111.9, 126.6, 150.2, 211.5; MS (ESI) m/z: 514 $[M]^+$. Anal. Calcd for $C_{25}H_{24}F_6N_2O_3$: C, 58.37; H, 4.70; N, 5.45. Found: C, 58.48; H, 4.47; N, 5.52.

(**4m**) 2,4-Bis(4-chlorophenyl)-10-(1,1-dioxa-2,2-dimethylene)-2,4-diazaspiro[5.5]undecan-7-one. White solid, (Yield: 61%); mp 132–134 °C; IR (KBr): 2954, 1708, 1512, 1456, 1244, 1042, 918, 826, 726 cm^{-1}; ^1H NMR (300 MHz, $CDCl_3$): δ 2.02 (t, J = 6.9 Hz, 2H), 2.11 (s, 2H), 2.58 (t, J = 6.9 Hz, 2H), 3.37 (d, J = 12.6 Hz, 2H), 3.85–3.74 (m, 4H), 3.93–3.88 (m, 2H), 4.08 (d, J = 11.1 Hz, 1H), 4.84 (d, J = 11.4 Hz, 1H), 6.98 (d, J = 9.0 Hz, 4H), 7.23 (d, J = 9.0 Hz, 4H), ^{13}C NMR (75 MHz, $CDCl_3$): 34.9, 36.3, 40.4, 48.7, 56.0, 64.4, 67.7, 106.9, 118.3, 125.2, 129.1, 148.4, 211.2; MS (ESI) m/z: 447 $[M]^+$. Anal. Calcd for $C_{23}H_{24}Cl_2N_2O_3$: C, 61.75; H, 5.41; N, 6.26. Found: C, 61.84; H, 5.47; N, 6.18.

(**4n**) 10-(1,1-Dioxa-2,2-dimethylene)-2,4-di-*p*-tolyl-2,4-diazaspiro[5.5]undecan-7-one. White Solid, (Yield: 52%); mp 126–128 °C; IR (KBr): 2928, 1710, 1522, 1108, 914, 734, 652 cm^{-1}; ^1H NMR (300 MHz, $CDCl_3$): δ 2.02 (t, J = 7.6 Hz, 2H), 2.16 (s, 2H), 2.27 (s, 6H), 2.62 (t, J = 6.6 Hz, 2H), 3.24 (d, J = 12.8 Hz, 2H), 3.79–3.72 (l, 4H), 3.88–3.82 (m, 2H), 3.93 (d, J = 11.1 Hz, 1H), 4.92 (d, J = 10.8 Hz, 1H), 6.98 (d, J = 8.6 Hz, 4H), 7.08 (d, J = 8.6 Hz, 4H), ^{13}C NMR (75 MHz, $CDCl_3$): 20.7, 35.3, 36.4, 40.1, 49.6, 56.4, 64.3, 69.7, 107.2, 117.4, 129.3, 149.7, 212.4; MS (ESI) m/z: 406 $[M]^+$. Anal. Calcd for $C_{25}H_{30}N_2O_3$: C, 73.86; H, 7.44; N, 6.89. Found: C, 73.75; H, 7.54; N, 6.74.

(**4o**) 2,4-Bis(3-chloro-4-fluorophenyl)-10-(1,1-dioxa-2,2-dimethylene)-2,4-diazaspiro[5.5] undecan-7-one. White solid, (Yield: 55%); mp 206–208 °C; IR (KBr): 2954, 1708, 1512, 1456, 1244, 1042, 918, 826, 726 cm^{-1}; ^1H NMR (300 MHz, $CDCl_3$): δ 2.09 (t, J = 7.5 Hz, 2H), 2.23 (s, 2H), 2.64 (t, J = 6.9 Hz, 2H), 3.38 (d, J = 12.3 Hz, 2H), 3.84–3.72 (m, 4H), 3.92–3.88 (m, 2H), 4.21 (d, J = 11.7 Hz, 1H), 4.85 (d, J = 11.7 Hz, 1H), 6.91 (s, 2H), 6.99 (d, J = 9.0 Hz, 2H), 7.29 (d, J = 9.0 Hz, 2H), ^{13}C NMR (75 MHz, $CDCl_3$): 24.6, 30.1, 37.1, 45.7, 54.1, 62.9, 64.8, 105.9, 118.2, 122.5, 128.1, 134.5, 138.5, 148.3, 211.3; MS (ESI) m/z: 483 $[M]^+$. Anal. Calcd for $C_{23}H_{22}Cl_2F_2N_2O_3$: C, 57.15; H, 4.59; N, 5.80. Found: C, 57.26; H, 4.70; N, 5.63.

3.5 Reusability of the catalyst

After completion of the reaction, 10 mL ethanol was added to the reaction mixture and the catalyst $CuFe_2O_4$ was separated magnetically, washed with ethanol and then air dried. The recovered catalyst was used directly in the next runs and no substantial loss of activity was observed up to four cycles.

4. Conclusion

In conclusion, we have developed a novel, green and highly efficient protocol for the synthesis of fluorine containing spirohexahydropyrimidine derivatives using magnetically separable and easily recyclable heterogeneous $CuFe_2O_4$ nanocatalyst in ethanol at room temperature. The magnetic nature of this heterogeneous nanocatalyst allows for its easy separation from the reaction mixture by using a simple bar magnet, which is an additional greener attribute of this reaction. Moreover, this method can be considered as an ideal tool for green synthesis because (1) rapid assembly of medicinally privileged heterocyclic molecules by a three-component process minimizes the generation of waste; (2) the process has high atom economy and environmentally benign, since

only water molecules are lost; (3) six covalent bonds are generated in a single reaction. Therefore, this one-pot, multicomponent procedure clearly represents an appealing methodology for the synthesis of highly substituted spiropyrimidines both in academia and pharmaceutical industries.

Acknowledgements

Financial assistance from the Council for scientific and Industrial Research New Delhi is gratefully acknowledged. We are thankful to the Bhabha Atomic Research Centre (BARC), Mumbai and Central Drug Research Institute (CDRI), Lucknow, for the spectral and elemental analyses. We are also thankful to STIC Cochin for single crystal X-ray analysis.

References

1 (*a*) B. C. Ranu, R. Dey, T. Chatterjee and S. Ahammed, *ChemSusChem*, 2012, **5**, 22; (*b*) S. B. Kalidindi and B. R. Jagirdar, *ChemSusChem*, 2012, **5**, 65; (*c*) R. Mout, D. F. Moyano, S. Rana and V. M. Rotello, *Chem. Soc. Rev.*, 2012, **41**, 2539; (*d*) A. Fihri, M. Bouhrara, B. Nekoueishahraki, J.-M. Basset and V. Polshettiwar, *Chem. Soc. Rev.*, 2011, **40**, 5181; (*e*) N. Tran and T. J. Webster, *J. Mater. Chem.*, 2010, **20**, 8760; (*f*) V. Polshettiwar and R. S. Varma, *Green Chem.*, 2010, **12**, 743; (*g*) V. Polshettiwar and R. S. Varma, *Chem. Soc. Rev.*, 2008, **37**, 1546; (*h*) J. Mondal, T. Sen and A. Bhaumik, *Dalton Trans.*, 2012, **41**, 6173; (*i*) T. Sen, I. J. Bruce and T. Mercer, *Chem. Commun.*, 2010, **46**, 6807.

2 Recent reviews and references therein: (*a*) V. Polshettiwar, R. Luque, A. Fihri, H. Zhu, M. Bouhrara and J.-M. Basset, *Chem. Rev.*, 2011, **111**, 3036; (*b*) S. Shylesh, V. Schunemann and W. R. Thiel, *Angew. Chem., Int. Ed.*, 2010, **49**, 3428; (*c*) A.-H. Lu, E. L. Salabas and F. Schuth, *Angew. Chem., Int. Ed.*, 2007, **46**, 1222.

3 (*a*) O. C. Agbaje, O. O. Fadeyi and C. O. Okoro, *Tetrahedron Lett.*, 2011, **52**, 5297; (*b*) R. Filler and R. Saha, *Future Med. Chem.*, 2009, **1**, 777; (*c*) C. Isanbor and D. O'Hagan, *J. Fluorine Chem.*, 2006, **127**, 303; (*d*) K. L. Kirk, *J. Fluorine Chem.*, 2006, **127**, 1013.

4 (*a*) L. Hunter, *Beilstein J. Org. Chem.*, 2010, **6**, 38; (*b*) D. O'Hagan, *Chem. Soc. Rev.*, 2008, **37**, 308.

5 T. Suzuki, T. Kubota and J. Kobayashi, *Bioorg. Med. Chem. Lett.*, 2011, **21**, 4220.

6 B. Renson, P. Merlin, D. Daloze, J. C. Braekman, Y. Roisin and J. M. Pasteels, *Can. J. Chem.*, 1994, **72**, 105.

7 K. Drandarov, A. Guggisberg and M. Hesse, *Helv. Chim. Acta*, 1999, **82**, 229.

8 A. Guggisberg, K. Drandarov and M. Hesse, *Helv. Chim. Acta*, 2000, **83**, 3035.

9 P. A. S. Smith and R. N. Loeppky, *J. Am. Chem. Soc.*, 1967, **89**, 1147.

10 A. Q. Siddiqui, L. Merson-Davies and P. M. Cullis, *J. Chem. Soc., Perkin Trans. 1*, 1999, 3243.

11 D. Hrvath, *J. Med. Chem.*, 1997, **40**, 2412 and the references therein.

12 R. J. Bergeron and H. W. Seligsohn, *Bioorg. Chem.*, 1986, **14**, 345.

13 (*a*) K. Chantrapromma, J. S. McManis and B. Ganem, *Tetrahedron Lett.*, 1980, **21**, 2475; (*b*) K. Chantrapromma and B. Ganem, *Tetrahedron Lett.*, 1981, **22**, 23; (*c*) I. A. Perillo, M. B. Garcia, J. A. Bisceglia and L. R. Orelli, *J. Heterocycl. Chem.*, 2002, **39**, 655; (*d*) A. R. Katrizky, S. K. Singh and H. Y. He, *J. Org. Chem.*, 2002, **67**, 3115; (*e*) M. Mayr and M. R. Buchmeiser, *Macromol. Rapid Commun.*, 2004, **25**, 231; (*f*) M. Mayr, K. Wurst, K. H. Ongania and M. R. Buchmeiser, *Chem.–Eur. J.*, 2004, **10**, 1256.

14 (*a*) S. Kambe, K. Saito, M. Hirose, A. Sakurai and H. Midorikawa, *Synthesis*, 1984, 860; (*b*) Z. J. Beresnevicius, V. Mickevicius, K. Rutkauskas and K. Kantminiene, *Polish J. Chem. Technol.*, 2003, **5**, 75.

15 (*a*) C. Mukhopadhyay, S. Rana and R. J. Butcher, *Tetrahedron Lett.*, 2011, **52**, 4153; (*b*) H.-L. Wei, Z.-Y. Yan, Y.-N. Niu, G.-Q. Li and Y.-M. Liang, *J. Org. Chem.*, 2007, **72**, 8600.

16 Recent review and references therein: (*a*) A. Domling, W. Wang and K. Wang, *Chem. Rev.*, 2012, **112**, 3083; (*b*) C. de Graaff, E. Ruijter and R. V. A. Orru, *Chem. Soc. Rev.*, 2012, **41**, 3969; (*c*) S. S. van Berkel, B. G. M. Bögels, M. A. Wijdeven, B. Westermann and F. P. J. T. Rutjes, *Eur. J. Org. Chem.*, 2012, 3543; (*d*) J. S. Yadav, A. Antony, J. George and B. V. S. Reddy, *Curr. Org. Chem.*, 2010, **14**, 414; (*e*) B. Jiang, F. Shi and S.-J. Tu, *Curr. Org. Chem.*, 2010, **14**, 357; (*f*) J. D. Sunderhaus and S. F. Martin, *Chem.–Eur. J.*, 2009, **15**, 1300.

17 (*a*) A. Dandia, A. K. Jain and S. Sharma, *Tetrahedron Lett.*, 2012, **53**, 5859; (*b*) A. Dandia, A. K. Jain and S. Sharma, *Tetrahedron Lett.*, 2012, **53**, 5270; (*c*) A. Dandia, A. K. Laxkar and R. Singh, *Tetrahedron Lett.*, 2012, **53**, 3012; (*d*) A. Dandia, R. Singh, S. Bhaskaran and S. D. Samant, *Green Chem.*, 2011, **13**, 1852; (*e*) A. Dandia, R. Singh and S. Bhaskaran, *Ultrason. Sonochem.*, 2011, **18**, 1113; (*f*) A. Dandia, A. K. Jain and D. S. Bhati, *Synth. Commun.*, 2011, **41**, 2905.

18 A. Dandia, V. Parewa, A. K. Jain and K. S. Rathore, *Green Chem.*, 2011, **13**, 2135.

19 A. Dandia, V. Parewa and K. S. Rathore, *Catal. Commun.*, 2012, **28**, 90.

20 J. E. Tasca, A. Ponzinibbio, G. Diaz, R. D. Bravo, A. Lavat and M. G. Gonzalez, *Top. Catal.*, 2010, **53**, 1087.

21 F. Davar and M. S. Niasari, *J. Alloys Compd.*, 2011, **509**, 2487.

22 (*a*) C. Poetra, *Environ. Health Perspect.*, 2004, **112**, a568; (*b*) S. Sabhi and J. Kiwi, *Water Res.*, 2001, **35**, 1994.

23 The crystal structure (**4k**: CCDC 897553) has been deposited at the Cambridge Crystallographic Data Center and is available on request from the Director, CCDC, 12 Union Road, Cambridge, CB2 1EZ, UK (Fax: +44-1223-336033; e-mail: deposit@ccdc.cam.ac.uk, http://www.ccdc.cam.ac.uk/deposit).

